# Influence of bed roughness on dune and megaripple generation

Déborah Idier,[1,2] Dominique Astruc,[3] and Suzanne J. M. H. Hulscher[1]

Received 12 March 2004; accepted 11 June 2004; published 10 July 2004.

[1] *Richards* [1980] conjectured that megaripples of the continental shelf are due to a seabed instability in the presence of seabed ripples. Towards a better understanding of this megaripple formation process, we use a morphodynamical numerical model to investigate the bed roughness influence on the bed load–induced linear stability of a sandy bed. We find that the linearly most amplified mode shifts from a dune mode (grain roughness) towards a megaripple mode (large bed roughness). Then, we discuss how megaripples could be generated over a flat bed and over dunes. *INDEX TERMS:* 3022 Marine Geology and Geophysics: Marine sediments—processes and transport; 4219 Oceanography: General: Continental shelf processes; 4255 Oceanography: General: Numerical modeling; 4512 Oceanography: Physical: Currents; 3045 Marine Geology and Geophysics: Seafloor morphology and bottom photography. **Citation:** Idier, D., D. Astruc, and S. J. M. H. Hulscher (2004), Influence of bed roughness on dune and megaripple generation, *Geophys. Res. Lett.*, *31*, L13214, doi:10.1029/2004GL019969.

## 1. Introduction

[2] Megaripples are dynamic continental shelf sedimentary structures with heights up to 2 m, wavelengths up to 20 m and crests perpendicular to the current (Table 1). They occur as rhythmic patterns and their migration rate may reach 1 m/h [*Idier et al.*, 2002]. They can be observed on flat beds as well as over large scale transverse bed forms, e.g., dunes [*Stride*, 1982]. Both dunes and megaripples are usually covered by even smaller bed forms, i.e., ripples. The prediction of the temporal evolution of the height and position of dunes and megaripples is of practical importance for various applications including navigation safety.

[3] As a first step towards the understanding of these bed forms dynamics, we focus on their generation processes. Linear stability analysis [*Richards*, 1980; *Hulscher*, 1996] showed that both dunes and ripples may result from free instabilities developing on the sandy interface between the seabed and the 3-dimensional current. Using the Navier-Stokes equations and a constant turbulent viscosity, *Hulscher* [1996] showed that the Linearly Most Amplified (LMA) mode has a wavelength similar to dunes wavelength observed in the field. *Richards* [1980] performed a similar analysis for a steady current using a depth-dependent turbulent viscosity model. He got two distinct unstable modes: one corresponding to ripples and the other corresponding to dunes. Increasing the bed roughness, the ripple mode wavelength increases whereas the dune mode wavelength decreases so that both modes coalesce for a critical value of the bed roughness. *Richards* [1980] conjectured that megaripples might be related to the ripple mode through a cascade process from ripples toward megaripples. However, none of these studies discuss in detail the generation of megaripples.

[4] In this letter, we study the generation of dunes and megaripples, focusing on 20 m wavelength megaripples as such features were observed in the Dover Strait [*Idier et al.*, 2002]. For this purpose, we use a numerical morphodynamical model taking into account bed load sediment transport only to study the linear regime of the bottom instability for various bed roughness heights.

## 2. Morphodynamical Model and Parameters

[5] In the present study we use a numerical model taking into account the free surface slope and based on a more sophisticated turbulence model than in previous stability analysis, as *Komarova and Hulscher* [2000] showed the benefits of turbulence modelling improvements. The flow model is based on the 3D hydrostatic Navier-Stokes equations. The vertical turbulent viscosity is parameterized by a mixing length model. A classical bottom friction parameterization is used:

$$\vec{\tau_b} = \rho \frac{\| \vec{u} \|^2}{C^2} \frac{\vec{u}}{\| \vec{u} \|} \quad \text{with} \quad C = (1/\kappa) \ln(\Delta Z / z_0) \tag{1}$$

where $\rho$ is the water density, $\vec{u}$ the near-bed velocity and $C$ the friction coefficient which depends on the Karman constant ($\kappa$ = 0.41), the bed roughness length $z_0$ and a characteristic length $\Delta Z$ (one tenth of the height of the first grid cell above the bottom [*Janin et al.*, 1997]). The bed roughness length $z_0$ is related to the bed roughness height $k_s$ by $z_0 = k_s/30$. $k_s$ is modelled as the sum of the grain roughness height $k_{bs}$ and the form roughness height $k_{bf}$:

$$k_s = k_{bs} + k_{bf} = 3\phi + 20 H_r^2 / \lambda_r \tag{2}$$

with $\phi$ the sediment grain size, $H_r$ and $\lambda_r$ the height and the wavelength of the small scale bed forms [*van Rijn*, 1989].

[6] The bottom evolution model is based on the sediment mass conservation, which relates the temporal bed evolution to the divergence of the sediment flux:

$$\frac{\partial h}{\partial t} + \frac{1}{1-\epsilon_p} \vec{\nabla}.\vec{S}_b = 0 \tag{3}$$

[1] Water Engineering and Management, University of Twente, Enschede, Netherlands.
[2] Now at Bureau de Recherches Géologiques et Minières, Orléans, France.
[3] Institut de Mécanique des Fluides de Toulouse, UMR 5502 CNRS-INPT-UPS, Toulouse, France.


0094-8276/04/2004GL019969$05.00

**Table 1.** Bed Form Classification and Associated Bed Roughness Height[a]

| | Ripples | Megaripples | Dunes |
|---|---|---|---|
| Height (m) | <0.06 | 0.06–2 | 2–15 |
| Wavelength (m) | <0.6 | 0.6–20 | 20–1000 |
| Roughness $k_s$ (m) | to 0.3 | 0.3 to 4 | 4 to 15 |

[a]From *Dalrymple et al.* [1978] and *van Rijn* [1989].

with $h$ the bed level, $\epsilon_p$ the bed porosity and $\vec{S}_b$ the sediment flux. Both bed load and gravity driven sediment fluxes are taken into account:

$$\vec{S}_b = \alpha(\| \vec{\tau}_b \| - \tau_c)^b \left( \vec{\tau}_b / \| \vec{\tau}_b \| - \beta \vec{\nabla} h \right) \quad (4)$$

$\tau_c$ is the critical bed shear stress, estimated with the *van Rijn* [1989] formula and $\beta$ is the bed slope coefficient, equal to the co-tangent of the repose angle of the sediment. $b$ and $\alpha$ are computed from the *van Rijn* [1989] formula:

$$b = 2.1 \quad \text{and} \quad \alpha = 0.053 \sqrt{(s-1)g} \phi^{1,5} D_*^{-0,3} \tau_c^{-2.1} \quad (5)$$

with $s = \rho_s/\rho$ the relative density, $D_* = \phi((s-1)g/\nu^2)^{1/3}$ the particle parameter and $\nu$ the water molecular viscosity.

[7] In this model, the grain size $\phi$ influences both the bed shear stress (1) and the sediment flux (5), whereas small-scale bed forms geometry (wavelength $\lambda_r$, height $H_r$) influences only the bed shear stress (1). To compute the flow, the sediment flux and the bed evolution, the Telemac finite element software is used, like in previous sandbanks studies [*Idier and Astruc*, 2003].

[8] As the spatial scales under consideration are small, the Coriolis force is neglected and the unstable modes crests are likely to be almost perpendicular to the current [*Hulscher*, 1996]. Thus, we use the 3D hydrodynamic model as a 2DV model (no lateral variability) and study the time evolution of small amplitude ($h$ = 15 cm) sinusoidal bed forms (wavelength $\lambda$) perpendicular to the current, superimposed to a flat bed, and subject to a steady flow (depth-averaged velocity $U$ = 1 m.s$^{-1}$, in the $x$-direction). The physical parameter values are those of dunes areas located in the Dover Strait: water depth $H$ = 30 m, grain size $\phi$ = 0.3 mm, $\beta$ = 1.3 (repose angle of 37.5°), $\rho_s$ = 2665 kg.m$^{-3}$, $\rho$ = 1000 kg.m$^{-3}$ and $\epsilon_p$ = 0.375. In the present study, no parameter tuning has been done to improve the model results. In the model, the vertical dimension $z$ is described by 10 logarithmically distributed layers, and the numerical errors are kept constant in all the computations (constant CFL number and 24 grid points per bed form wavelength).

[9] From the initial and final bathymetry computed with the numerical model, we estimate the complex growth rate $\omega$ of the bed perturbations, as $\partial \tilde{h}_1/\partial t = \omega \tilde{h}_1$ with $\tilde{h}_1(x, t)$ the Fourier Transform of the first order bed perturbation. The bed perturbation growth rate is the real part of $\omega$ and the migration rate is $\lambda Im(\omega)/2\pi$. Each point $(\lambda, z_0)$ of Figure 1 corresponds to one numerical computation performed for a bed perturbation $h_1(x, t)$ of wavelength $\lambda$ and a bed roughness $z_0$.

## 3. Results: From Dunes to Megaripples

[10] First, for a ripple-free bed ($z_0$ = 0.003 cm), among the studied wavelength range [10 m–500 m], a single LMA mode ($\lambda$ = 400 m) is observed (Figure 1) which lies in the range [100 m–600 m] of observed dunes in the south of the North Sea [*Stride*, 1982]. In addition, the small wavelength perturbations ($\lambda$ < 175 m) are damped.

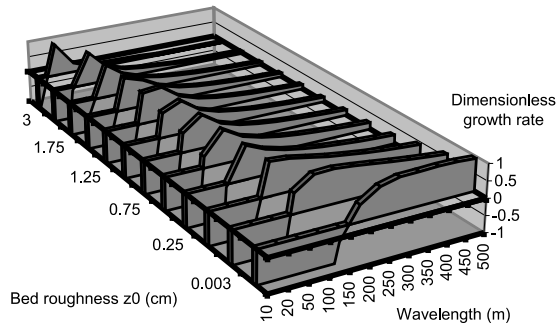


**Figure 1.** Scaled growth rate versus bed roughness length $z_0$. (The growth rate is scaled by the growth rate of the LMA mode obtained for each bed roughness value).

[11] Subsequently, computations are performed to analyze whether small-scale bed forms such as megaripples may grow if ripples are present on the sandy bed (as conjectured by *Richards* [1980]). For that purpose, the bed form-related roughness height $k_{bf}$ is included in the bed roughness $k_s$. Figure 1 shows that, increasing $k_s$, the LMA mode shifts towards the short wavelengths. The 20 m wavelength megaripple observed on Dover Strait dunes [*Idier et al.*, 2002] is found to be the LMA mode for a bed roughness length of 3.6 cm (i.e., $k_s$ = 1.1 m) (Figure 1). The continuous decrease of the wavelength, from dunes to megaripples, suggests that the generation mechanisms of dunes and megaripples are similar within the limits of this model. An appealing comment on this result is that it fits the classification of bottom bed forms proposed by *Ashley* [1990] on the basis of field observations in which the wavelength of the so-called dunes extends from 0.6 to 1000 m with no distinction between dunes and megaripples whereas at smaller scales, ripples are distinguished.

[12] Figure 2 shows that the megaripple growth and migration rates are several orders of magnitude larger than those of the dunes: small bed forms are more dynamic than larger ones. From observations in the Dover Strait [*Idier et al.*, 2002], the dune (160 m width) migrates of about 10 m/y (including meteorological effects), whereas the overlapping megaripples ($\lambda \sim 20$ m) have a migration up to 5 m per tidal cycle (12.42 h) (for a period of quiet weather). Thus, the ratio $R$ between dune migration rate and megaripple migra-

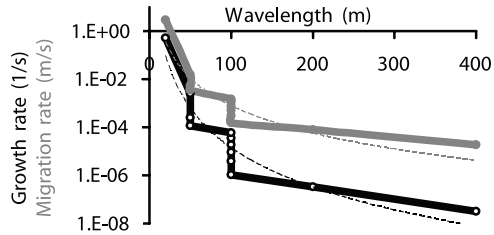


**Figure 2.** Dimensional growth and migration rates versus the wavelength of the LMA modes. The dotted lines are interpolation of the discrete LMA modes we obtained.

tion rate is 400. Using the model results for wavelengths of 160 and 20 m (Figure 2), we find $R = 2600$. This ratio is 6 times larger than the ratio obtained from field observations. This discrepancy should be related to the model assumptions (dunes perpendicular to the current, small amplitude dynamics, hydrostatic pressure) and to the fact that in the field, the dune migration rate is estimated over one year (due to the slow dynamics) whereas the megaripple migration rate is estimated over a single tide.

## 4. Hydrodynamics and Bed Form Generation

[13] In this paragraph, using the above numerical results and some algebra, we analyze the relation between hydrodynamics, bed slope effect and bed form generation.

[14] For the analysis purpose, we split the bed shear stress in two parts: one ($\tau_{b0}$) corresponding to the bed shear stress over a flat bed, the other one ($\tau_{b1}$) corresponding to the perturbation due to the presence of the bottom structures. $\tau_{b1} = |\tau_{b1}| \cos(2\pi x/\lambda + \varphi_{\tau_b})$ with $\varphi_{\tau_b}$ the spatial phase-lag between the bathymetry and the bed shear stress (a positive phase-lag means a maximum bed shear stress upstream of the dune crest).

[15] From *Richards* [1980], the sign of the growth rate is controlled by the balance between a term $A$ proportional to $|\tau_{b1}|\sin\varphi_{\tau_b}$ and a damping term $B$ (always negative). This damping term is proportional to the bedslope coefficient $\beta$ and to the bottom perturbation wave number and is independent of the bed roughness. Using equation (1) and a Fourier transform, we estimate $\tau_{b0}$, $|\tau_{b1}|$ and $\varphi_{\tau_b}$ from our numerical computations (Figure 3). The phase-lag $\varphi_{\tau_b}$ is always positive, lower than $\pi$. Thus the term $A$ is always positive and is a growth term. Figure 3 shows that for increasing bed roughness, $\tau_{b0}$, $|\tau_{b1}|$ and $\sin\varphi_{\tau_b}$ increase leading to a growth term increase. Physically, a bed roughness increase leads to an increase of the vertical turbulent diffusion and thus of the bed shear stress ($\tau_{b0}$) and the free surface slope, but also of $|\tau_{b1}|$ and $\varphi_{\tau_b}$ [*Dawson et al.*, 1983]. Further more, $|\tau_{b1}|$ decreases with the wavelength, whereas $\sin\varphi_{\tau_b}$ increases, such that $|\tau_{b1}|\sin\varphi_{\tau_b}$ is non-monotonous and reaches a maximum, which is shifted towards the shorter wavelength for increasing bed roughness. Adding the effects of the A and B terms of the growth rate, the results of Figure 1 are recovered: the LMA mode wavelength decreases for increasing bed roughness (due to the shift of the maximum of A) whereas the short wavelength damped modes band becomes narrower (due to the imbalance between increasing A and constant B terms for increasing bed roughness).

## 5. Discussion

[16] In this section, we propose some mechanisms to explain the generation in the field of megaripples over a flat bed and over dunes. The underlying assumption of this discussion is that it is relevant to compare the LMA mode to finite amplitude dunes and megaripples observed in the field. Indeed, even if such comparison is not rigorously justified, we should notice that some studies ([*Calvete et al.*, 2001] for sandridges) found that the LMA mode is the dominant mode in the non-linear regime.

[17] According to our numerical computations ($H = 30$ m and $U = 1$ m/s), the bed roughness height required for 20 m wavelength megaripple to be the LMA mode over a flat bed is $k_{sc} = 1.1$ m. This value is higher than the grain (0.09 cm) or ripple (max. 0.3 m) induced bed roughness height. Thus grain or ripple induced bed roughness only cannot explain the large bed roughness $k_{sc}$ which is responsible for the presence of megaripples. In this discussion, we focus on the mechanisms responsible for such large bed roughness on a flat bed and then over a dune. One should notice that even if some suspended transport should occur under this large bottom shear stress ($\tau_{b0} = 125$ kg/m/s; Figure 3a), in this preliminary study, only bed load–induced bed evolution is considered.

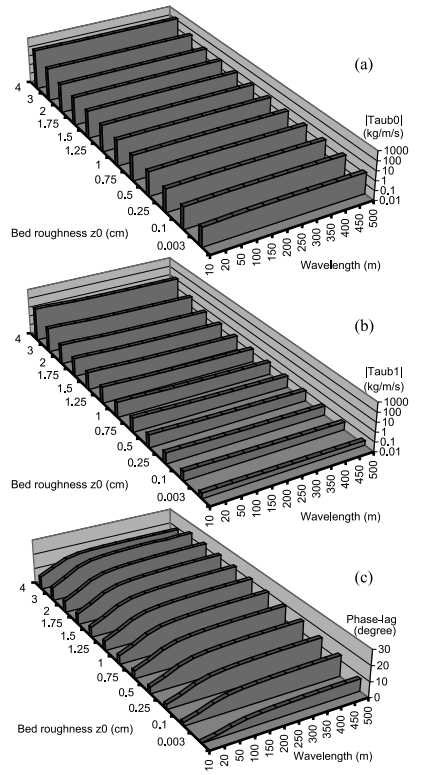


**Figure 3.** Numerical results: (a) 0-order bed shear stress modulus $|\tau_{b0}|$, (b) First order bed shear stress modulus $|\tau_{b1}|$, (c) Phase-lag $\varphi_{\tau_b}$ of the first order bed shear stress with respect to the bathymetry.

### 5.1. Megaripple Generation Over a Flat Bed

[18] The computed critical bed roughness height $k_{sc} = 1.1$ m over a flat bed (equation (2)) is almost equal to the height of observed 20 m wavelength megaripples (about 1 m). This coincidence is intriguing. However, within the framework of the present morphodynamical model, no clear conclusions can be drawn as the sub-grid-scale bottom features which are parameterized by means of the bed roughness cannot be distinguished from the resolved megaripples. The investigation deserved to clarify this point is out of the scope of this letter.

[19] In addition to grain and ripple induced bed roughness, the presence of surface waves in shallow waters can lead to an apparent bed roughness 1 to 10 (depending on the water depth and surface wave characteristics) times larger than the physical roughness [*Perlin and Kit*, 2002]. In the present study (30 m water depth and for a depth-averaged

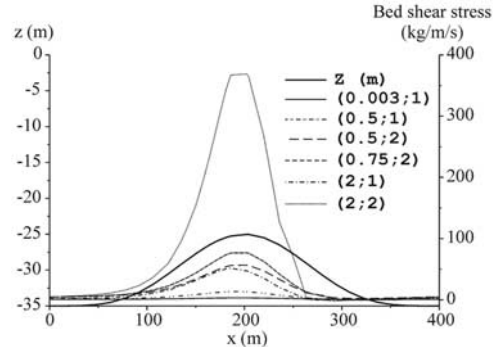


**Figure 4.** Bed shear stress profile over a finite amplitude dune, located in the middle of a periodic dune field, for different sets of ($z_0$ in cm, $U$ in m.s$^{-1}$).

flow velocity of 1 m.s$^{-1}$), surface waves would lead to an apparent grain (resp. ripple) roughness height up to 0.9 cm (resp. 3 m), the latter being larger than the critical $k_{sc}$ value so that megaripples can be generated by the combined roughness enhancement of ripples and surface waves.

### 5.2. Megaripple Generation Over Dunes

[20] Dunes are also often covered by megaripples. The megaripples height may be constant [*Terwindt*, 1971] or increasing along the dune profile [*Idier et al.*, 2002], the former case being the most common.

[21] Field measurements [*Dyer*, 1970] and modelling studies [*Dawson et al.*, 1983] show that the bed shear stress increases along the stoss side of dunes. This increase is not only due to an increase of the depth-integrated velocity $U$ by water mass conservation, but also to a flow acceleration, which can be related to an apparent bed roughness (equation (1)) such that a similar velocity profile can be obtained over a flat bed if this apparent bed roughness is considered. Thus, assuming that the megaripple wavelength (20 m) is small compared to the dune wavelength (160 m) and that the dune bed position variations are small over a megaripple wavelength, we can use the results obtained for a flat bed to estimate whether megaripple can grow over a given dune.

[22] A situation ($k_s \leq k_{sc}$) where 20 m wavelength megaripple are damped over a flat bed is selected to study the effect of a dune on the bed shear stress distribution with the help of the flow model. The dunes superimposed to the flat bottom (in 35 m water depth) have a trochoidal shapes ($\sin^4$ wave) like observed dunes, a height of 10 m and a wavelength of 400 m (Figure 4). Hydrodynamic computations are performed for various couples of bed roughness $z_0$ and depth-averaged velocity $U$ values (Figure 4).

[23] The presence of the dune leads to bed shear stress values larger than the corresponding value for dune-free bottom (whatever the bed roughness and the depth-averaged velocity values are) at the exception of a small region downstream of the dune where the value is smaller and possibly negative (Figure 4). A maximum bed shear stress of 360 kg/m/s is reached at the dune crest for the couple $z_0$ = 2 cm (i.e., $k_s$ = 0.6 m) and $U$ = 2 m/s which is 72 times larger than its value upstream of the dune (5 kg/m/s). This velocity value is representative of the current in the dune area studied by *Idier et al.* [2002]. The contribution of mass conservation to this bed shear stress enhancement proved to only doubles it. Thus the contribution of the apparent roughness related to the flow acceleration over the dune is dominant. From the bed shear stress value at the crest and upstream the dune, the apparent bed roughness height at the crest is estimated to be $k_s$ = 1.2 m. This value exceeds the $k_{sc}$ = 1.1 m critical value obtained for a flat bed.

[24] Thus, a possible conclusion is that dune slopes support megaripple generation by combined action of the dune itself, small ripples and moderate surface waves. This could explain why the feet of the dune and the area in between the dunes may remain megaripple-free as only longwave perturbations can develop. This result still hold for sand starved areas [*Idier et al.*, 2002] where in between the dunes the coarser sediment related bed roughness remains behind the critical value.

## 6. Conclusion

[25] This study of the seabed stability shows that for increasing bed roughness the linearly most amplified mode shifts from a dune mode of 400 m wavelength (grain roughness) towards a megaripple mode of 20 m wavelength (bed roughness height $k_s$ of about 1 m). Thus, megaripples would emerge as a combined action of ripples and wave. Various mechanisms are proposed to explain the origin of the large bed roughness height required for the megaripple generation. They could explain the observed full covering of the sea bed by megaripples (combined action of ripples and surface waves) and the partial dunes covering (combined action of dunes, ripples and surface waves). However, the present study includes only the bed load transport and neglects suspended sediment transport. It could be worthwhile to investigate the influence of such an assumption on the present results.

[26] **Acknowledgments.** The authors would like to thank the French Hydrographic Service (SHOM), the CNRS, STW and the European project EUMARSAND for financial support. The reviewers are gratefully acknowledged for their fruitful comments and suggestions.

## References

Ashley, G. M. (1990), Classification of large-scale subaqueous bedforms: A new look at an old problem, *J. Sediment. Petrol.*, *60*, 160–172.

Calvete, D., M. Walgreen, H. E. de Swart, and A. Falques (2001), A model for sand ridges on the shelf: Effect of tidal and steady currents, *J. Geophys. Res.*, *106*, 9311–9325.

Dalrymple, R. W., R. J. Knoght, and J. J. Lambiase (1978), Bedforms and their hydraulic stability relationship in a tidal environment, Bay of Fundy, Canada, *Nature*, *275*, 100–104.

Dawson, G. P., B. Johns, and R. L. Soulsby (1983), A numerical model of shallow-water flow over topography, in *Physical Oceanography of Coastal and Shelf Seas*, edited by B. Johns, *Elsevier Oceanogr. Ser.*, *35*, 267–320.

Dyer, K. R. (1970), Current velocity profiles in a tidal channel, *Geophys. J. R. Astron. Soc.*, *22*, 153–161.

Hulscher, S. J. M. H. (1996), Tidal-induced large-scale regular bed form patterns in a three-dimensional shallow-water model, *J. Geophys. Res.*, *101*(C9), 20,727–20,744.

Idier, D., and D. Astruc (2003), Analytical and numerical modeling of large-scale rhythmic bedform dynamics, *J. Geophys. Res.*, *108*(C3), 3060, doi:10.1029/2001JC001205.

Idier, D., A. Ehrhold, and T. Garlan (2002), Morphodynamics of an undersea sandwave of the Dover Strait, *C. R. Geosci.*, *334*, 1079–1085.

Janin, J. M., F. Marcos, and T. Denot (1997), Code Telemac-3D-version 2.2, *Tech. Rep. E-42/97/049/B*, Electr. de France, Lab. Natl. d'Hydraul., Chatou, France.

Komarova, N. L., and S. J. M. H. Hulscher (2000), Linear instability mechanisms for sand wave formation, *J. Fluid Mech.*, *413*, 219–246.

Perlin, A., and E. Kit (2002), Apparent roughness in wave-current flow: Implication for coastal studies, *J. Hydraul. Eng.*, 729–741.

Richards, K. (1980), The formation of ripples and dunes on an erodible bed, *J. Fluid Mech.*, *99*, 597–618.

Stride, A. H. (1982), *Offshore Tidal Sands*, chap. 3, Chapman and Hall, New York.

Terwindt, J. H. J. (1971), Sand waves in the Southern Bight of the North Sea, *Mar. Geol.*, *10*, 51–67.

van Rijn, L. C. (1989), *Handbook of Sediment Transport by Currents and Waves*, 1002 pp., Delft Hydraul., Delft, Netherlands.

D. Astruc, Institut de Mécanique des Fluides de Toulouse, UMR 5502 CNRS-INPT-UPS, Allée Pr. C. Soula, F-31400 Toulouse, France.

S. J. M. H. Hulscher, Water Engineering and Management, University of Twente, P.O. Box 217, NL-7500 AE, Enschede, Netherlands.

D. Idier, Bureau de Recherches Géologiques et Minières, 3 Av. C. Guillemin, 45060 Orléans cedex 2, France. (d.idier@brgm.fr)